RESEARCH ARTICLE
doi: 10.2306/scienceasia1513-1874.2022.080

ScienceAsia 48 (2022): **596–604**

In vitro cytotoxic activity, molecular docking study, and chemical composition of *Zingiber cassumunar* root oil

Pongsit Vijitphan, Arthit Makarasen*, Suwicha Patnin, Decha Dechtrirat, Peerada Yingyuad, Supanna Techasakul*

Department of Chemistry, Laboratory of Organic Synthesis, Chulabhorn Research Institute, Bangkok 10210 Thailand

*Corresponding authors, e-mail: arthit@cri.or.th, supanna@cri.or.th

Received 3 Aug 2021, Accepted 7 Feb 2022
Available online 25 May 2022

ABSTRACT: The cytotoxic activities against cancer cell lines of eight known sesquiterpene and phenylbutenoids, namely, (−)-β-sesquiphellandrene (1), (*E*)-1-(3,4-dimethoxyphenyl)buta-1-ene (2), (*E*)-1-(3,4-dimethoxyphenyl)buta-1,3-diene (3), (*E*)-1-(2,4,5-trimethoxyphenyl)buta-1-ene (4), (*E*)-1-(2,4,5-trimethoxyphenyl)buta-1,3-diene (5), (*E*)-4-(3,4-dimethoxyphenyl)buta-3-eneyl acetate (6), (±)-*trans*-3-(3,4-dimethoxyphenyl)-4-[(*E*)-3,4-dimethoxystyryl]cyclohex-1-ene (7), and (±)-*cis*-3-(3,4-dimethoxyphenyl)-4-[(*E*)-3,4-dimethoxystyryl]cyclohex-1-ene (8) were evaluated. All compounds were isolated from the rhizomes of *Zingiber cassumunar* Roxb. (Plai) using classical column chromatography. Compounds 1, 7, and 8 exhibited good cytotoxic activity against acute lymphoblastic leukemia (MOLT-3) with half maximal inhibitory concentration (IC_{50}) values of 16.39 ± 1.22, 16.41 ± 3.68, and 14.38 ± 0.78 μg/ml; promyelocytic leukemia (HL-60) with IC_{50} values of 7.64 ± 0.33, 15.25 ± 0.88, and 13.02 ± 0.91 μg/ml; and hormone-independent breast cancer (MDA-MB-231) with IC_{50} values of 27.71 ± 1.41, 28.99 ± 2.30, and 27.94 ± 2.24 μg/ml, respectively. Compounds 3, 7, and 8 displayed good anticancer activity against cervical carcinoma (HeLa) with IC_{50} values of 18.68 ± 0.62, 20.86 ± 1.68, and 18.89 ± 1.26 μg/ml, respectively. The results showed that two diastereomers (7 and 8) have good activity against the broad range of tested cancer cell lines. From molecular docking analysis, the binding energy and interaction between the isolated compounds and topoisomerase II (Top2) was calculated and could be used to evaluate cytotoxic activity. Molecular docking showed that 7 and 8 interacted with Top2 (α and β types) using two or three hydrogen bonding, whereas the other compounds that also displayed this interaction had at least one hydrogen bonding. Additionally, only 7 exhibited non-toxic effect against normal embryonic lung cell line (MRC-5); therefore, the biological activity of 7 can serve as a basis for the study of anti-cancer agents in the near future.

KEYWORDS: *Zingiber cassumunar*, cytotoxicity, sesquiterpene, phenylbutenoid, molecular docking

INTRODUCTION

The Zingiberaceae plant family commonly found in Southeast Asia is known for its medicinal, pharmacological, and nutritional properties. *Zingiber cassumunar* Roxb., a plant in the Zingiberaceae family known as "Plai" or "Wan-fai", is used as traditional medicine to relieve pain, flatulence, and asthma [1–4]. Essential oil from the rhizomes of *Z. cassumunar* Roxb. has a wide variety of biological activities, such as antibacterial [5, 6], antimicrobial [7], anti-inflammatory [8, 9], antioxidant [10], anticoagulant [11], anticancer [12], and insecticidal effects [13]. Additionally, phytochemicals from Plai essential oil have been investigated as well. The major components that can be isolated from this plant, including terpenes, phenylbutenoids, and curcuminoids, depend on the crude preparation methods, such as solvent extraction and distillation [14]. Most of the isolated components also exhibit good biological activities. For example, curcuminoid groups have strong antioxidant activity [15], and phenylbutenoids exhibit good anti-inflammatory activity [16]. Nowadays, cancer is a major cause of deaths around the world. Cancer treatment procedures include surgery, radiation therapy, and chemotherapy. In chemotherapy, patients receive chemotherapeutic drugs that target and eradicate cancer cell lines. Nevertheless, chemotherapeutic drugs also affect regular cells and cause many undesirable adverse effects, such as nausea, vomiting, and hair loss [17]. Currently available commercial chemotherapeutic drugs are slightly expensive and can be carcinogenic [18, 19]. Therefore, the discovery of new anticancer drugs is very important to prevent the drug resistance of cancer cell lines and reduce the side effects of chemotherapeutic agents. Natural products have served as a productive source for novel drug discovery, particularly anticancer drugs [20]. Almost half of the drugs approved in the previous decade are based on natural products [21, 22]. In addition, over one-third of therapeutic drugs derived from natural products in all pharmaceutical development stages are cancer treatment agents. Thus, the exploration of new natural products for drug development is highly recommended. In this work, we reported the isolation of eight known secondary metabolites from Plai oil via classical liquid column chromatography. The ^{1}H and ^{13}C nuclear magnetic resonance (NMR) spectroscopy and mass spectroscopy of all the isolated compounds from Plai oil were elucidated. The results corresponded with previous reports [23–25] in which these compounds were separated by high-performance

liquid chromatography (HPLC). However, the spectroscopic data of some compounds are not clear, and only few studies have reported the cytotoxic activity of the sesquiterpene and phenylbutenoids isolated in the present study against cancer cell lines. We also used molecular docking to predict the binding sites, binding energy, and interaction of the assigned compounds and biological molecules.

Herein, the completed reports on the spectroscopic data along with the cytotoxic activity and molecular docking study of the isolated compounds were evaluated and accomplished. The phytochemicals were tested for cytotoxic activity against ten normal and drug-resistant cancer cell lines and normal embryonic lung cell line (MRC-5). The study could contribute to the discovery of effective anticancer drugs.

MATERIALS AND METHODS

Cell lines, chemicals, and biochemicals

MOLT-3 (acute lymphoblastic leukemia), HuCCA-1 (cholangiocarcinoma), A549 (lung carcinoma), HepG2 (hepatocarcinoma), MRC-5 (normal embryonic lung cell), HeLa (cervical carcinoma), T47-D (hormone-dependent breast cancer), H69AR (lung cancer, multidrug resistance), S102 (Thai liver cancer), MDA-MB-231 (hormone-independent breast cancer), and HL-60 (promyelocytic leukemia) cell lines were either purchased from the American Type Culture Collection (ATCC, Manassas, VA, USA) or received as gifts from other sources. Dulbecco's Modified Eagle Medium (DMEM), as well as Ham's F12 and RPMI 1640 media, were supplied in powder form by HyClone Laboratories (Logan, UT, USA), while fetal bovine serum (FBS) and 0.25% trypsin-EDTA were obtained from JR Scientific, Inc. (Woodland, CA, USA) and Gibco (Grand Island, NY, USA), respectively. In addition, bovine insulin, DMSO, doxorubicin, etoposide, glucose, l-glutamine, MTT (3-(4,5-dimethylthiazol-2-yl)-2,5-diphenyltetrazoliumbromide), penicillin-streptomycin, phenazine methosulfate (PMS), and sodium pyruvate were supplied by Sigma-Aldrich (St. Louis, MO, USA), whereas XTT (2,3-bis-(2-methoxy-4-nitro-5-sulfophenyl)-2H-tetrazolium-5-carboxanilide) was from Fluka Chemie (St. Louis, MO, USA).

Plant materials

The rhizomes of *Z. cassumunar* Roxb. were purchased from a local market in Bangkok, Thailand in September 2020. The voucher specimen (TTM-1000644) was deposited to Thai Traditional Medicine Herbarium, Department of Thai Traditional and Alternative Medicine, Ministry of Public Health, Bangkok, Thailand. The fresh rhizomes of *Z. cassumunar* Roxb. were washed and cut into small pieces before steam distillation using Clevenger apparatus. The Plai essential oil was kept in a dark bottle with light protection under N_2 atmosphere at 4 °C.

Phytochemicals from Plai oil

The crude essential oil from *Z. cassumunar* Roxb. (9.1058 g) was subjected to classical liquid chromatography (column dimensions: 4×50 cm, flowrate: 10 ml/min) on silica gel 60 (0.063–0.200 mm; 70–230 mesh ASTM; Merck, Darmstadt, Germany) using *n*-hexane and ethyl acetate (EtOAc) as the mobile phase. The gradient eluent with increasing polarity was as follows 95:5, 2500 ml; 90:10, 2000 ml, 85:15, 1000 ml; 80:20, 1000 ml; 75:25, 1000 ml; and 70:30, 500 ml. The fractions of Plai (FP) were collected based on a thin-layer chromatography pattern and concentrated to give seven fractions, FP1 to FP7. Each fraction was combined, concentrated, and identified: the lowest polar fraction, FP1 (colorless oil, 1276.5 mg, 14.0% yield) as (−)-β-sesquiphellandrene (1); FP2 (light yellow oil, 364.2 mg, 4.0% yield) as (*E*)-1-(3,4-dimethoxyphenyl)buta-1-ene (2); FP3 (light yellow oil, 658.3 mg, 7.2% yield) as (*E*)-1-(3,4-dimethoxyphenyl)buta-1,3-diene (3); FP4 (yellow oil, 22.0 mg, 0.24% yield) as (*E*)-1-(2,4,5-trimethoxyphenyl)buta-1-ene (4); FP5 (yellow oil, 84.2 mg, 0.92% yield) as (*E*)-1-(2,4,5-trimethoxyphenyl)buta-1,3-diene (5); FP6 (yellow oil, 16.5 mg, 0.18% yield) as (*E*)-4-(3,4-dimethoxyphenyl)buta-3-eneyl acetate (6); and lastly, FP7 (a pale brown solid, 489.0 mg, 5.4% yield). ^{1}H and ^{13}C NMR spectroscopy data indicated that FP7 could be a mixture of phenylbutenoid diastereomers. A classical liquid column chromatography (column dimensions: 2.5×20 cm, flowrate: 1 ml/min) of FP7 was conducted on silica gel 60 (< 0.063 mm; Merck) using isocratic elution with dichloromethane-EtOAc (98.5:2.5, 1000 ml) to obtain two subfractions of FP7, namely, FP7-1 and FP7. These two subfractions were collected and elucidated as two known cyclohexene derivatives: (±)-*trans*-3-(3,4-dimethoxyphenyl)-4-[(*E*)-3,4-dimethoxystyryl]cyclohex-1-ene (7) as colorless needles (223.1 mg, 2.5% yield) and (±)-*cis*-3- (3,4-dimethoxyphenyl)-4-[(*E*)-3,4-dimethoxystyryl]cyclohex-1-ene (8) as pale yellow solid (127.8 mg, 1.4% yield).

Structure characterization

The melting points were measured using an SMP3 Stuart™ digital melting point apparatus from Bibby Sterlin, Ltd (Staffordshire, UK). To confirm the structure, the products were analyzed by nuclear magnetic resonance (NMR) and mass spectrometry. Proton and carbon NMR spectra were obtained using the Bruker AvanceIII-HD-400 spectrometer at 400 and 100 MHz, respectively. High-resolution mass spectra were measured with an ESI-TOF, i.e., MicroTOF mass spectrometer (Bruker Daltonics, Germany). The optical rotation was measured using a Jasco P-1020 Polarimeter (Tokyo, Japan). The spectroscopic data were also compared with previous reports, and the valid results

of all compounds were herein summarized.

(−)-β-sesquiphellandrene (1): $[\alpha]_D^{28}$–4.77° ($CHCl_3$; *c* 1.00); ^{1}H—NMR (400 MHz, $CDCl_3$): 0.84 (d, 3H, J = 6.8 Hz), 1.14–1.24 (m, 1H), 1.33–1.44 (m, 2H), 1.50–1.58 (m, 1H), 1.60 (s, 3H), 1.69 (s, 3H), 1.70–1.75 (m, 1H), 1.90–1.99 (m, 1H), 1.99-2.06 (m, 1H), 2.20–2.24 (m, 1H), 2.27–2.31 (m, 1H), 2.44 (dt, 1H, J = 14.8, 4.0 Hz), 4.73 (s, 1H), 4.75 (s, 1H), 5.10 (tt, 1H, J = 7.2, 1.2 Hz), 5.67 (d, 1H, J = 10.0 Hz), 6.14 (dd, 1H, J = 10.0, 2.4 Hz); 13C-NMR (100 MHz, $CDCl_3$): 15.8, 17.6, 24.4, 25.7, 26.0, 30.3, 34.2, 36.6, 40.5, 109.8, 124.7, 129.5, 131.2, 135.2, 143.7; ESI-MS (Positive ion mode) m/z for $C_{15}H_{25}$ found 205.1951 = $[M + H]^+$ (calcd. 205.1951).

(*E*)-1-(3,4-dimethoxyphenyl)buta-1-ene (2): ^{1}H-NMR (400 MHz, $CDCl_3$): 1.09 (t, 3H, J = 8.0 Hz), 2.23 (qn, 2H, J = 8.0 Hz), 3.87 (s, 3H), 3.90 (s, 3H), 6.14 (dt, 1H, J = 16.0, 8.0 Hz), 6.32 (d, 1H, J = 16.0 Hz), 6.80 (d, 1H, J = 8.0 Hz), 6.87 (dd, 1H, J = 8.0, 2.0 Hz), 6.91 (d, 1H, J = 2.0 Hz); ^{13}C-NMR (100 MHz, $CDCl_3$): 13.7, 26.0, 55.7, 55.9, 108.4, 111.1, 118.7, 128.4, 130.7, 131.1, 148.1, 148.9; ESI-MS (Positive ion mode) m/z for $C_{12}H_{17}O_2$ found 193.1224 = $[M + H]^+$ (calcd. 193.1223).

(*E*)-1-(3,4-dimethoxyphenyl)buta-1,3-diene (3): ^{1}H-NMR (400 MHz, $CDCl_3$): 3.88 (s, 3H), 3.91 (s, 3H), 5.13 (d, 1H, J = 9.6 Hz), 5.30 (dd, 1H, J = 16.4, 1.6 Hz), 6.44–6.49 (m, 1H), 6.51–6.53 (m, 1H), 6.67 (dd, 1H, J = 15.2, 10.8 Hz), 6.82 (d, 1H, J = 8.0 Hz), 6.93–6.96 (m, 2H); ^{13}C-NMR (100 MHz, $CDCl_3$): 55.6, 55.7, 108.6, 111.0, 116.5, 119.7, 127.7, 130.1, 132.5, 137.1, 148.8, 148.9; ESI-MS (Positive ion mode) m/z for $C_{12}H_{15}O_2$ found 191.1071 = $[M + H]^+$ (calcd. 191.1067).

(*E*)-1-(2,4,5-trimethoxyphenyl)buta-1-ene (4): ^{1}H-NMR (400 MHz, $CDCl_3$): 1.10 (t, 3H, J = 7.2 Hz), 2.24 (qnd, 2H, J = 7.6, 1.6 Hz), 3.82 (s, 3H), 3.87 (s, 3H), 3.88 (s, 3H), 6.12 (dt, 1H, J = 16.0, 6.8 Hz), 6.50 (s, 1H), 6.64 (d, 1H, J = 16.0 Hz), 6.97 (s, 1H); ^{13}C-NMR (100 MHz, $CDCl_3$): 13.9, 26.4, 56.1, 56.5, 56.7, 98.0, 109.6, 118.9, 122.8, 131.3, 143.4, 148.7, 150.7; ESI-MS (Positive ion mode) m/z for $C_{13}H_{19}O_3$ found 223.1328 = $[M + H]^+$ (calcd. 223.1329).

(*E*)-1-(2,4,5-trimethoxyphenyl)buta-1,3-diene (5): ^{1}H-NMR (400 MHz, $CDCl_3$): 3.84 (s, 3H), 3.88 (s, 3H), 3.90 (s, 3H), 5.10 (d, 1H, J = 10.0 Hz), 5.28 (d, 1H, J = 16.8 Hz), 6.50 (s, 1H), 6.48–6.57 (m, 1H), 6.68 (dd, 1H, J = 15.6, 10.0 Hz), 6.86 (d, 1H, J = 15.6 Hz), 7.00 (s, 1H); ^{13}C-NMR (100 MHz, $CDCl_3$): 56.0, 56.5, 56.7, 97.7, 109.4, 116.0, 118.0, 127.1, 128.0, 138.0, 143.4, 149.6, 151.6 ; ESI-MS (Positive ion mode) m/z for $C_{13}H_{17}O_3$ found 221.1172 = $[M + H]^+$ (calcd. 221.1172).

(*E*)-4-(3,4-dimethoxyphenyl)buta-3-eneyl acetate (6): ^{1}H-NMR (400 MHz, $CDCl_3$): 2.06 (s, 3H), 2.53 (qd, 2H, J = 6.8, 1.2 Hz), 3.88 (s, 3H), 3.90 (s, 3H), 4.18 (t, 2H, J = 6.8 Hz), 6.03 (dt, 1H, J = 16.0, 6.8 Hz), 6.41 (d, 1H, J = 16.0 Hz), 6.81 (d, 1H, J = 8.0 Hz) 6.87–6.91 (m, 2H); ^{13}C-NMR (100 MHz, $CDCl_3$): 21.0, 32.3, 55.8, 55.9, 63.8, 108.6, 111.1, 119.1, 123.6, 130.4, 132.0, 148.6, 149.0, 171.1; ESI-MS (Positive ion mode) m/z for $C_{14}H_{18}NaO_4$ found 273.1096 = $[M + Na]^+$ (calcd. 273.1097).

(±)-*trans*-3-(3,4-dimethoxyphenyl)-4-[(*E*)-3,4-dimethoxystyryl]cyclohex-1-ene (7): ^{1}H-NMR (400 MHz, $CDCl_3$): 1.66–1.72 (m, 1H), 1.90–1.96 (m, 1H), 2.20–2.22 (m, 2H), 2.32–2.39 (m, 1H), 3.17–3.20 (m, 1H), 3.82 (s, 3H), 3.85 (s, 3H), 3.86 (s, 3H), 3.87 (s, 3H), 5.68 (dd, 1H, J = 10.0, 2.4 Hz), 5.88–5.92 (m, 1H), 6.01 (dd, 1H, J = 16.0, 6.8 Hz), 6.10 (d, 1H, J = 16.0 Hz), 6.70–6.81 (m, 6H); ^{13}C-NMR (100 MHz, $CDCl_3$): 24.5, 27.8, 45.4, 48.0, 55.8, 55.8, 55.9, 108.7, 110.8, 111.1, 111.6, 118.8, 120.4, 127.6, 128.8, 130.2, 130.9, 132.2, 137.5, 147.3, 148.2, 148.6, 148.9; mp. 81.0–83.0 °C [22]; ESI-MS (Positive ion mode) m/z for $C_{24}H_{29}O_4$ found 381.2056 = $[M + H]^+$ (calcd. 381.2060).

(±)-*cis*-3-(3,4-dimethoxyphenyl)-4-[(*E*)-3,4-dimethoxystyryl]cyclohex-1-ene (8): ^{1}H-NMR (400 MHz, $CDCl_3$): 1.61–1.68 (m, 2H), 2.19–2.23 (m, 2H), 2.67–2.75 (m, 1H), 3.51 (bs, 1H), 3.75 (s, 3H), 3.83 (s, 3H), 3.85 (s, 3H), 3.86 (s, 3H), 5.59 (dd, 1H, J = 15.6, 9.2 Hz), 5.78–5.82 (m, 1H), 5.97–5.99 (m, 1H), 6.25 (d, 1H, J = 15.6 Hz), 6.69–6.81 (m, 6H); ^{13}C-NMR (100 MHz, $CDCl_3$): 24.3, 24.8, 42.6, 45.7, 55.7, 55.8, 55.9, 108.6, 110.3, 111.1, 113.6, 118.7, 121.9, 128.0, 128.5, 129.1, 131.0, 132.4, 133.8, 147.5, 148.1, 148.2, 148.9; mp. 98.0–99.5 °C [22]; ESI-MS (Positive ion mode) m/z for C24H29O4 found 381.2057 = $[M + H]^+$ (calcd. 381.2060).

Cytotoxic activity

All materials were used as received. Among the 10 cancerous and 1 normal cell lines used for cytotoxicity screening of compounds, 9 cell lines were adherent to the culture wells, whereas only HL-60 and MOLT-3 grew in suspension. Each cell line was maintained in an appropriate culture medium supplemented with essential nutrients and maintained using standard procedures at 37 °C with 95% humidity and 5% CO_2. All the test compounds and positive controls, including doxorubicin and etoposide, were prepared as 10 mg/ml stock solutions in DMSO and freshly diluted with the corresponding cell culture medium for each cell line on the day of analysis.

Prior to the assay, the cells were inoculated as a suspension in the corresponding cell culture medium (100 ml for adherent cells and 75 ml for suspended cells) into 96-well microtiter plates (Costar No. 3599, Corning Incorporated, Corning, NY, USA) at a density of 5000–20 000 cells per well, depending on their growth rates. Adherent and suspended cells were then allowed to grow at 37 °C with 95% humidity and 5% CO_2 for 24 h and 30 min, respectively. The cytotoxicity

assay was initiated by adding an equal volume of cell culture medium containing either each test compound, positive control, or DMSO, at predetermined concentrations. Following 48 h of exposure to various treatments, cell viability was determined using MTT assay for adherent cells or XTT assay for suspended cells, as described below.

For adherent cells, 100 ml of the MTT reagent (0.5 mg/ml in serum-free cell culture medium) was added to each well, and the microtiter plates were further incubated for 2.5–4 h at 37 °C with 95% humidity and 5% CO_2 [26, 27]. The medium was subsequently replaced with 100 ml of DMSO to dissolve the purple formazan before the absorbance at 550 nm was measured using a Spectra-Max Plus 384 microplate reader (Molecular Devices, Sunnyvale, CA, USA) with a reference wavelength of 650 nm.

For suspended cells, 75 ml of the XTT reagent (prepared from 5 ml of 1 mg/ml XTT sodium in water and 100 ml of 0.383 mg/ml PMS in water) was added to each well, and the cells were further incubated for 4 h at 37 °C with 95% humidity and 5% CO_2 [28]. Afterwards, the absorbance of orange formazan at 492 nm was measured with a reference wavelength of 690 nm using a SpectraMax Plus 384 microplate reader. For each well, the background absorbance (averaged from the wells containing the same volume of complete culture medium) was subtracted from either A550 or A492 to get the absolute absorbance. The average value from the duplicate wells, which had been treated with each concentration of the test compounds, was then compared with that of the untreated wells to yield the percentage of surviving cells.

The half maximal inhibitory concentrations (IC_{50} value) was finally calculated from the dose-response curve as the concentration that inhibits the cell growth by 50% in comparison with the negative control following 48 h of exposure to each test compound.

Molecular docking

Molecular docking can be used to study the binding energy of small ligand on the enzyme. The geometry of ligands was fully optimized using the density functional theory (DFT) at B3LYP/6-31G (d, p) level implemented in Gaussian 09. The crystal structures of topoisomerase IIα (Top2α) (PDB Id: 4FM9) and (PDB Id: 3QX3) for Top2β are obtained from the Protein data bank. The binding interactions of ligands with Top2 are simulated via molecular docking using Autodock 4.2 [29]. The grid box size of 60, 60, and 60 along the X, Y and Z axes with a grid-point spacing of 0.375 Å was applied for molecular docking. The center of grid for Top2 was set to 50.093, 40.387 and 14.321 Å for Top2α and 42.855, 96.185 and 48.248 Å for Top2β [30]. The docking parameter simulations were performed with 150 runs, 2.5×10^6 energy evaluations and 27 000 number of generations. The molecular docking results can be explained by BIOVIA Discovery Studio 2020.

RESULTS AND DISCUSSION

The isolated metabolites consisted of one sesquiterpene and seven phenylbutenoids from *Z. cassumunar* Roxb., namely, (−)-*β*-sesquiphellandrene (1) [31], (*E*)-1-(3,4-dimethoxyphenyl)buta-1-ene (2) [23], (*E*)-1-(3,4-dimethoxyphenyl)buta-1,3-diene (3) [32], (*E*)-1-(2,4,5-trimethoxyphenyl)buta-1-ene (4), (*E*)-1-(2,4,5-trimethoxyphenyl)buta-1,3-diene (5) [33], (*E*)-4-(3,4-dimethoxyphenyl)buta-3-eneyl acetate (6) [34], (±)-*trans*-3-(3,4-dimethoxyphenyl)-4-[(*E*)-3,4-dimethoxystyryl]cyclohex-1-ene (7), and (±)-*cis*-3-(3,4-dimethoxyphenyl)-4-[(*E*)-3,4-dimethoxystyryl]cyclohex-1-ene (8) [34]. The structures of all isolated compounds were demonstrated in Fig. 1. Diastereomers 7 and 8 are difficult to separate [25, 34]. Nevertheless, 7 and 8 were easily isolated in the present study by normal column chromatography using silica gel 60 as the stationary phase. The structures of the isolated compounds were displayed and confirmed by ^{1}H and ^{13}C NMR spectroscopy and mass spectroscopy (Fig. 1, Supplementary data: Fig. S3–S10 and Table S1–S4). The isolated compounds (1–8) were tested for cytotoxic activity against four normal cancer cell lines (MOLT-3, HuCCA-1, A549, and HepG2) and normal embryonic lung cell line (MRC-5). The results are tabulated in Table 1. Compounds 1–8 exhibited good cytotoxic activity against acute lymphoblastic leukemia (MOLT-3). Particularly, compounds 1, 7, and 8 had the IC_{50} values of 16.39 ± 1.22, 16.41 ± 3.68, and 14.38 ± 0.78 μg/ml, respectively. The other compounds displayed moderate anticancer activity against MOLT-3 with IC_{50} values in the range of 30–36 μg/ml. Additionally, 1–8 showed poor cytotoxic activity against cholangiocarcinoma (HuCCA-1), lung carcinoma (A549), and hepatocarcinoma cell lines (HepG2) except for compound 5, which illustrated strong activity against HepG2 with an IC_{50} value of 17.83 ± 4.14 μg/ml. More than half of the tested compounds exhibited no harmful effect against normal embryonic lung cells (MRC-5) except compounds 1, 3, and 8, which had IC_{50} values of 30–31 μg/ml. Compounds 1–8 were also tested for cytotoxic activity against human malignant and drug-resistant cancer cell lines (HeLa, T47-D, H69AR, S102, MDA-MB-231, and HL-60), and the results (Table 2) showed that all the tested compounds displayed moderate to high cytotoxic activity against cervical carcinoma cell line (HeLa) with IC_{50} values in the range of 18–44 μg/ml except for 6. Phenylbutenoids 3, 7, and 8 showed good cytotoxicity against HeLa with IC_{50} values of 18.68 ± 0.62, 20.86 ± 1.68, and 18.89 ± 1.26 μg/ml, respectively. Moreover, 1 exhibited the highest

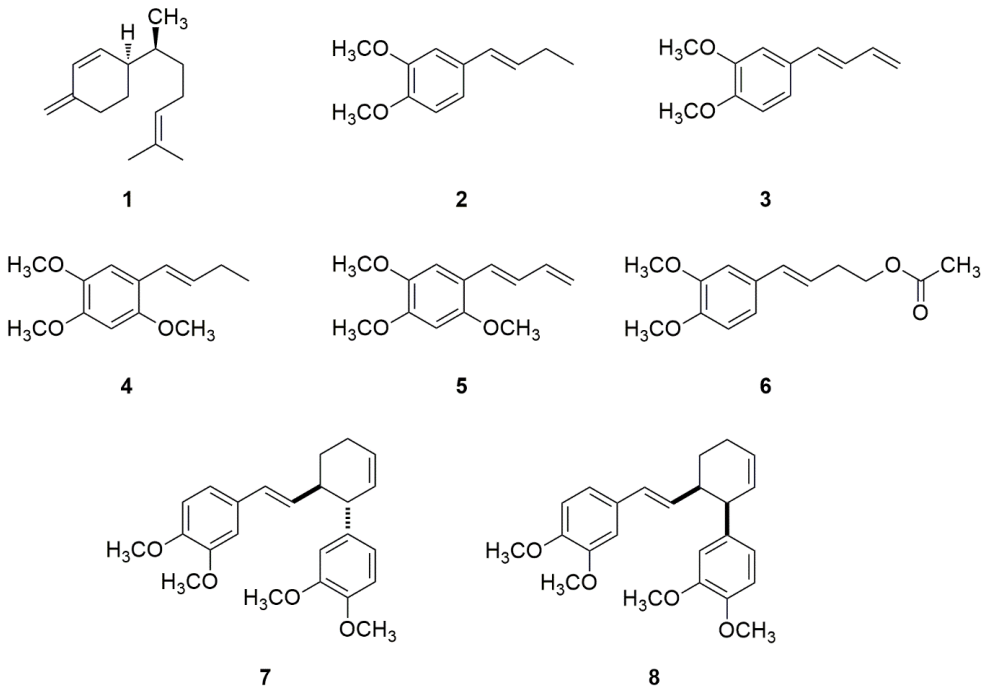

Fig. 1 Chemical structures of (−)-β-sesquiphellandrene (1), (*E*)-1-(3,4-dimethoxyphenyl)buta-1-ene (2), (*E*)-1-(3,4-dimethoxyphenyl)buta-1,3-diene (3), (*E*)-1-(2,4,5-trimethoxyphenyl)buta-1-ene (4), (*E*)-1-(2,4,5-trimethoxyphenyl)buta-1,3-diene (5), (*E*)-4-(3,4-dimethoxyphenyl)buta-3-eneyl acetate (6), (±)-*trans*-3-(3,4-dimethoxyphenyl)-4-[(*E*)-3,4-dimethoxystyryl]cyclohex-1-ene (7) and (±)-*cis*-3-(3,4-dimethoxyphenyl)-4-[(*E*)-3,4-dimethoxystyryl]cyclohex-1-ene (8).

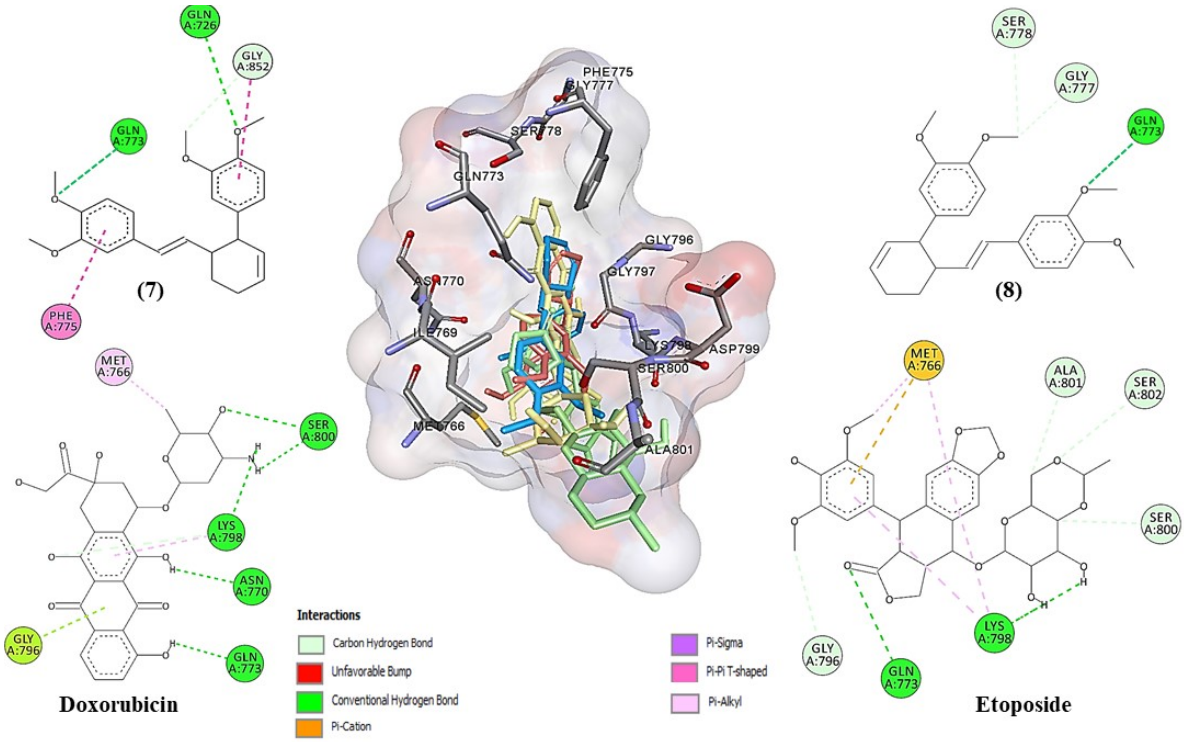

Fig. 2 The binding interaction between the ligands ((7): yellow, (8): green, (Doxorubicin): blue, (Etoposide): red) and Top2α as revealed from molecular docking.

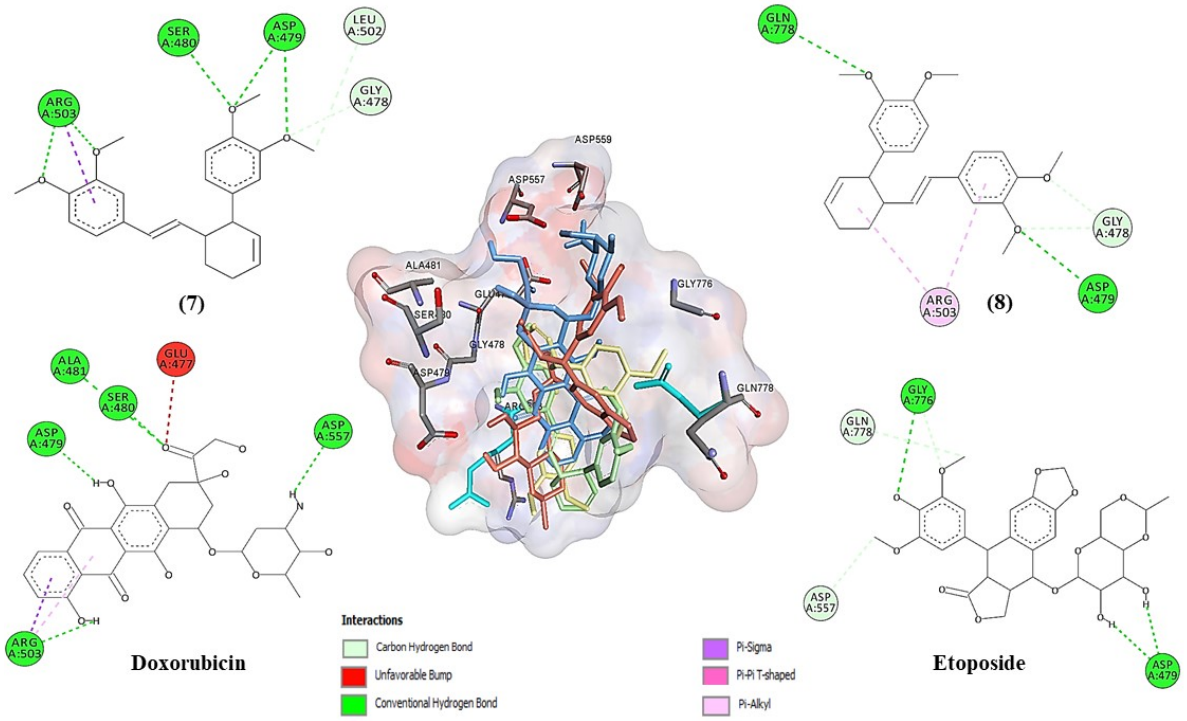

Fig. 3 The binding interaction between the ligands ((7): yellow, (8): green, (Doxorubicin): blue, (Etoposide): red) and Top2β as revealed from molecular docking.

Table 1 *In vitro* cytotoxic activity of compounds 1–8 against human cancer cell lines.

Compound	Cell line [IC_{50} (μg/ml)]				
	MOLT-3	HuCCA-1	A549	HepG2	MRC-5
1	16.39 ± 1.22	%C = 45	44.06 ± 1.53	27.00 ± 1.13	30.76 ± 4.20
2	30.35 ± 4.66	%C = 43	%C = 35	%C = 31.73	%C = 35.43
3	31.09 ± 2.33	%C = 19	%C = 5	27.05 ± 1.90	30.94 ± 2.80
4	31.35 ± 0.14	%C = 5	%C = 28	%C = 33.50	%C = 41.10
5	35.49 ± 0.83	%C = 2	%C = 15	17.83 ± 4.14	%C = 34.30
6	33.29 ± 0.50	Inactive	Inactive	%C = 21.56	%C = 5.10
7	16.41 ± 3.68	%C = 7	%C = 43	%C = 46.15	Inactive
8	14.38 ± 0.78	42.32 ± 1.15	36.64 ± 2.64	33.07 ± 1.82	30.40 ± 1.88
Doxorubicin	0.008 ± 0.001	0.58 ± 0.044	0.33 ± 0.049	0.36 ± 0.02	1.31 ± 0.13
Etoposide	0.017 ± 0.001	–	–	36.71 ± 1.78	–

MOLT-3 (acute lymphoblastic leukemia), HuCCA-1 (cholangiocarcinoma), A549 (lung carcinoma), HepG2 (hepatocarcinoma), MRC-5 (normal embryonic lung cell). Results are expressed as mean ± standard error of inhibition perceptual for all cell lines. Doxorubicin and etoposide were used as positive control. Experiments were performed in triplicate. IC_{50} values were obtained from 10 μg/ml concentration of substance; %C = % inhibition at the 50 μg/ml concentration of substance; inactive (IC_{50} > 50 μg/ml; %C = 0).

cytotoxic activity against hormone-dependent breast cancer (T47-D), lung cancer multidrug resistance (H69AR), Thai liver cancer (S102), and hormone-independent breast cancer (MDA-MB-231) cell lines with IC_{50} values of 18.32 ± 0.35, 38.67 ± 0.38, 29.57 ± 0.95, and 27.71 ± 1.41 μg/ml, respectively. Moreover, 1–8 also demonstrated moderate to severe cytotoxicity against promyelocytic leukemia (HL-60) with IC_{50} values in the range of 13–46 μg/ml. Particularly, compounds 1, 5, 7, and 8 showed strong activity against HL-60 with IC_{50} values of 7.64 ± 0.33, 19.20 ± 2.72, 15.25 ± 0.88, and 13.02 ± 0.91 μg/ml, respectively.

The result of the cytotoxicity assay revealed that 1, 7, and 8 had potential cytotoxicity against MOLT-3 and HL-60 with low IC_{50} values. Both cell lines are part of leukemia, which is a type of cancer that occurs in the bone marrow caused by the abnormal growth of white

Table 2 *In vitro* cytotoxic activity of compounds 1–8 against human malignant and drug resistance human cancer cell lines.

Compound	Cell line [IC_{50} (μg/ml)]					
	HeLa	T47-D	H69AR	S102	MDA-MB-231	HL-60
1	33.01 ± 1.15	18.32 ± 0.35	38.67 ± 0.38	29.57 ± 0.95	27.71 ± 1.41	7.64 ± 0.33
2	30.92 ± 1.70	%C = 39	Inactive	%C = 1.58	%C = 46.60	29.51 ± 1.20
3	18.68 ± 0.62	%C = 43	Inactive	%C = 18.96	%C = 30.65	24.74 ± 7.60
4	44.12 ± 0.18	44.66 ± 0.261	Inactive	%C = 22.86	%C = 35.74	37.15 ± 1.34
5	31.00 ± 0.08	%C = 48	%C = 3	%C = 13.94	%C = 24.66	19.20 ± 2.72
6	%C = 33	%C = 39	Inactive	%C = 9.42	%C = 15.98	46.19 ± 6.28
7	20.86 ± 1.68	27.04 ± 2.906	Inactive	Inactive	28.99 ± 2.30	15.25 ± 0.88
8	18.89 ± 1.26	39.25 ± 0.212	%C = 47	33.36 ± 2.41	27.94 ± 2.24	13.02 ± 0.91
Doxorubicin	0.28 ± 0.03	0.41 ± 0.04	25.00 ± 0.00	0.99 ± 0.04	1.18 ± 0.07	0.07 ± 0.01
Etoposide	–	–	–	–	–	0.39 ± 0.07

HeLa (cervical carcinoma), T47-D (hormone-dependent breast cancer), H69AR (lung cancer, multidrug resistance), S102 (Thai liver cancer), MDA-MB-231 (hormone-independent breast cancer), HL-60 (promyelocytic leukemia). Results are expressed as mean ± standard error of inhibition perceptual for all cell lines. Doxorubicin and etoposide were used as positive control. Experiments were performed in triplicate. IC_{50} values were obtained from 10 μg/ml concentration of substance; %C = % inhibition at the 50 μg/ml concentration of substance; inactive (IC_{50} > 50 μg/ml; %C = 0).

Table 3 Binding energy and H-bonding interaction between ligands (compounds 1–8, doxorubicin and etoposide) and Top2(α&β).

Ligand	Binding energy (kcal/mol) with Top2α	H-bonding interaction with Top2α	Binding energy (kcal/mol) with Top2β	H-bonding interaction with Top2β
1	−6.93 ± 0.12	–	−5.99 ± 0.04	–
2	−5.85 ± 0.05	–	−4.72 ± 0.09	ARG503
3	−5.96 ± 0.04	–	−4.77 ± 0.11	–
4	−5.97 ± 0.08	–	−4.81 ± 0.04	GLN778
5	−6.05 ± 0.15	–	−4.86 ± 0.13	GLN778
6	−6.73 ± 0.03	–	−5.23 ± 0.10	–
7	−8.46 ± 0.17	GLN726 GLN773 ASN770	−7.54 ± 0.15	ASP479 SER480 ARG503
8	−8.12 ± 0.26	GLY788 GLN773	−7.31 ± 0.24	ASP479 GLN778
Doxorubicin	−8.81 ± 0.19	GLN773 ASN770 SER800 LYS798	−9.74 ± 0.18	ASP479 SER480 ALA481 ARG503 ASP557
Etoposide	−7.74 ± 0.21	ASN774 PHE790 GLY791	−9.84 ± 0.27	ASP479 GLY776

blood cells. Leukemia can be treated with radiation therapy, chemotherapy, and bone marrow transplant. Chemotherapy is the primary method of treatment for leukemia. The chemotherapy drugs currently used to treat leukemia are the anthracycline class, such as doxorubicin and daunorubicin [35, 36]. Doxorubicin and etoposide are powerful anticancer drugs that block DNA replication by inhibiting the mechanism of action of DNA topoisomerase II (Top2) [37, 38]. Top2 is an enzyme that controls the supercoiling of DNA; plays a key role in replication, translation, recombination, and segregation in the cell cycle; and is used as a marker for cancer cells. In mammals, Top2 can be divided into two isoforms, namely, Top2α and Top2β. Top2α is involved in DNA replication whereas Top2β plays an important role in the survival of some neurons [39, 40]. The binding interactions among Top2α/β, the tested compounds, and commercial chemotherapy drugs (doxorubicin and etoposide) were studied by molecular docking approach [29, 30]. In this work, molecular docking may be used to explain the binding mechanisms of isolated compounds with Top2α/β and their cytotoxicity against cancer cell lines. The binding energy values and binding interaction between the ligands and Top2α/β were calculated and are presented in Fig. 2, Fig. 3 and Table 3. The lowest binding energy value was found in doxorubicin with values of −8.81 ± 0.19 kcal/mol for Top2α and etoposide with values of −9.74 ± 0.18 kcal/mol for Top2β. In the case of Top2α, phenylbutenoids 7 and 8 also demonstrated low binding energy values similar to that of doxorubicin and lower than that of etoposide with value

of -8.46 ± 0.17 and -8.12 ± 0.26 kcal/mol, respectively. Compounds 1–6 displayed high binding energy values and did not have H-bonding interaction with Top2α/β possibly because of the small molecular size and characteristics of hydrocarbons. The molecular docking results showed that the binding interactions between all analyzed compounds and Top2α/β in the binding pocket were within the radius of 5.0 Å (Fig. 2, 3, Supplementary data: Fig. S1 and S2). The hydrogen bonding interactions between phenylbutenoids (7 and 8) and Top2α/β were found in the amino acid residues GLN773 for Top2α and ASP479 for Top2β as demonstrated in Fig. 2 and Fig. 3. GLN773 and ASP479 also interacted with doxorubicin and etoposide via hydrogen bonding interactions with Top2α and Top2β, respectively. In addition, the other interactions occurred between ligands and amino acid residues such as carbon hydrogen bond, pi-alkyl, and pi-sigma. Docking study suggested that the compounds (7, 8), doxorubicin, and etoposide bound in a binding pocket with H-bonding interactions through the methoxy group, carbonyl group, and hydroxyl group in the side chain of ligands. The results displayed that phenylbutenoids 7 and 8 bound in the pockets of Top2α and Top2β to a similar area as those of doxorubicin and etoposide. The crucial pharmacophores in the compounds 7 and 8 that interacted to Top2α and Top2β are dimethoxyphenyl groups. The O atoms in dimethoxyphenyl side chain can form H-bonding interaction with amino acid residues on Top2α and Top2β. These are significant groups that related to core skeleton of doxorubicin and etoposide which displayed H-bonding interaction. The cytotoxicity against cancer cell lines of doxorubicin demonstrated lower IC_{50} value than that of compound 7 whereas the binding energy of doxorubicin and compound 7 with Top2 showed similar value. The result implied that doxorubicin may be involved in other enzymes or process in the inhibition of cancer cell lines. However, Top2 is one of several enzymes involved in the functioning of cancer cells. In previous report using molecular docking analysis, the binding interaction between anticancer drugs and Top2 revealed that GLN726 and GLN773 in Top2α and ASP479 and ARG503 in Top2β are important key points for anticancer drugs [33]. Thus, our results from molecular docking study corresponded to the cytotoxic activity against cancer cell lines, particularly MOLT-3 and HL-60. Therefore, 7 and 8 showed potential as Top2 inhibitors for the development of anticancer drugs in the near future.

CONCLUSION

The essential oil obtained from *Z. cassumar* contained potential constituents with strong cytotoxic activity against leukemia cancer cell lines, namely, acute lymphoblastic leukemia (MOLT-3) and promyelocytic leukemia (HL-60) cell lines. The sesquiterpene (1) and two cyclohexene diasteromers (7 and 8) showed high cytotoxicity against MOLT-3 and HL-60. However, only compound 7 exhibited no harmful effect against normal embryonic lung cells (MRC-5) with IC_{50} value of > 50 μg/ml; thus, 7 may be a potent novel anticancer drug. Molecular docking demonstrated that the O atoms in dimethoxyphenyl side chain of 7 and 8 interacted with amino acid residues of Top2 (α and β types) through two or three hydrogen bonds. Compounds 7 and 8 bound in the pockets of Top2α and Top2β to a similar area as those of doxorubicin and etoposide.

Appendix A. Supplementary data

Supplementary data associated with this article can be found at http://dx.doi.org/10.2306/scienceasia1513-1874.2022.080.

Acknowledgements: The authors are grateful to Chulabhorn Research Institute and and Thailand Science Research and Innovation (TSRI) for financial support (Grant No. 2536708/41859). We also acknowledge the Thai Traditional Medicine Herbarium, Department of Thai Traditional and Alternative Medicine for the voucher specimen.

REFERENCES

1. Chongmelaxme B, Sruamsiri R, Dilokthornsakul P, Dhippayom T, Kongkaew C, Saokaew S, Chuthaputti A, Chaiyakunapruk N (2017) Clinical effects of *Zingiber cassumunar* (Plai): a systematic review. *Complement Ther Med* **35**, 70–77.
2. Wolff XY, Astuti IP, Brink M (1999) Zingiber GR Boehmer, In: deGuzman CC, Siemonsma JS (eds) *Plant Resources of South-East Asia (PROSEA)*, Backhuys Publishers, Leiden, The Netherlands, pp 233–238.
3. Sharifi-Rad M, Varoni EM, Salehi B, Sharifi-Rad J, Matthews KR, Ayatollahi SA, Kobarfard F, Ibrahim SA, et al (2017) Plants of the genus *Zingiber* as a source of bioactive phytochemicals: from tradition to pharmacy. *Molecules* **22**, 2145–2164.
4. Anasamy T, Abdul AB, Sukari MA, Abdelwahab SI, Mohan S, Kamalidehghan B, Azid MZ, Nadzri NM, et al (2013) A phenylbutenoid diner, cis-3-(3′,4′-dimethoxyphenyl)-4-[(*E*)-3‴,4‴-dimethoxystyryl] cyclohex-1-ene, exhibits apoptogenic properties in T-acute lymphoblastic leukemia cells via induction of p53-independent mitochondrial signaling pathway. *Evid-Based Complementary Altern Med* **2013**, ID 939810.
5. Boonyanugomol W, Kraisriwattana K, Rukseree K, Boonsam K, Narachai P (2017) *In vitro* synergistic antibacterial activity of the essential oil from *Zingiber cassumunar* Roxb against extensively drug-resistance *Acinetobacter baumannii* strains. *J Infect* **10**, 586–592.
6. Verma RS, Joshi N, Padalia RC, Singh VR, Goswami P, Verma SK, Iqbal H, Chanda D, et al (2018) Chemical composition and antibacterial, antifungal, allelopathic and acethycholinesterase inhibitory activites of cassumunar-ginger. *J Sci Food Agric* **98**, 321–327.
7. Pithayanukul P, Tubprasert J, Wuthi-Udomlert M (2007) *In vitro* antimicrobial activity of *Zingiber cassumunar* (Plai) oil and a 5% Plai oil gel. *Phytother Res* **21**, 164–169.

8. Ozaki Y, Kawahara N, Harada M (1991) Anti-inflammatory effect of *Zingiber cassumunar* ROXB. and its active principles. *Chem Pharm Bull* **39**, 2353–2356.
9. Kaewchoothong A, Tewtrakul S, Panichayupakaranant P (2012) Inhibitory effect of phenylbutanoid-rich *Zingiber cassumunar* extracts on nitric oxide production by murine macrophage-like RAW264.7 cells. *Phytother Res* **26**, 1789–1792.
10. Saeio K, Chaiyana W, Okonogi S (2011) Antityrosinase and antioxidant activities of essential oils of edible Thai plants. *Drug Discov Ther* **5**, 144–149.
11. Sukati S, Jarmkom K, Techaoei S, Wisidsri N, Khobjai W (2019) *In vitro* anticoagulant and antioxidant activities of Prasaplai recipe and *Zingiber cassumunar* Roxb. extracts. *Int J App Pharm* **11**, 26–30.
12. Taechowisan T, Suttichokthanakorn S, Phutdhawong WS (2018) Antibacterial and cytotoxicity activities of phenylbutanoids from *Zingiber cassumunar* Roxb. *J Appl Pharm Sci* **8**, 121–127.
13. Nugroho BW, Schwarz B, Wray V, Proksch P (1996) Insecticidal constituents from rhizomes of *Zingiber cassumunar* and *Kaempferia rotunda*. *Phytochemistry* **41**, 129–132.
14. Amatayakul T, Cannon JR, Dampawan P, Dechatiwongse T, Giles RGF, Huntrakul C, Kusamran K, Mokkhasamit M, et al (1979) Chemistry and crystal structures of some constituents of *Zingiber cassumunar*. *Aust J Chem* **32**, 71–88.
15. Jitoe A, Masuda T, Tengah IGP, Suprapta DN, Gara IW, Nakatani N (1992) Antioxidant activity of tropical ginger extracts and analysis of the contained curcuminoids, *J Agric Food Chem* **40**, 1337–1340.
16. Jeenapongsa R, Yoovathaworn K, Sriwatanakul KM, Pongprayoon U, Sriwatanakul K (2003) Anti-inflammatory activity of (*E*)-1-(3,4-dimethoxyphenyl) butadiene from *Zingiber cassumunar* Roxb. *J Ethnopharmacol* **87**, 143–148.
17. Pearce A, Haas M, Viney R, Pearson S-A, Haywood P, Brown C, Ward R (2017) Incidence and severity of self-reported chemotherapy side effects in routine care: a prospective cohort study. *PLoS One* **12**, e0184360.
18. Harris CC (1976) The carcinogenicity of anticancer drugs: a hazard in man. *Cancer* **37**, 1014–1023.
19. Blagosklonny MV (2005) Carcinogenesis, cancer therapy and chemoprevention, *Cell Death Differ* **12**, 592–602.
20. Charoenwongpaiboon T, Laowtammathron C, Lorthongpanich C (2021) Therapeutic opportunities for cancers presented by natural and synthetic compounds targeting the Hippo signaling pathway. *ScienceAsia* **47**, 665–672.
21. Newman DJ, Cragg GM, Snader KM (2003) Natural products as sources of new drugs over the period 1981–2002. *J Nat Prod* **66**, 1022–1037.
22. Harvey AL (2008) Natural product in drug discovery. *Drug Discov Today* **13**, 894–901.
23. Kuroyanagi M, Fukushima S, Yoshihara K, Natori S, Dechatiwongse T, Mihashi K, Nishi M, Hara S (1980) Further characterization of the constituents of a Thai medicinal plant, *Zingiber cassumunar* ROXB. *Chem Pharm Bull* **28**, 2948–2959.
24. Nakamura S, Iwami J, Matsuda H, Wakayama H, Pongpriyadacha Y, Yoshikawa M (2009) Structures of new phenylbutanoids and nitric oxide production inhibitors from the rhizomes of *Zingiber cassumunar*. *Chem Pharm Bull* **57**, 1267–1272.
25. Jitoe A, Masuda T, Nakatani N (1993) Phenylbutenoid dimers from the rhizomes of *Zingiber cassumunar*. *Phytochemistry* **32**, 357–363.
26. Mosman T (1983) Rapid colorimetric assay for cellular growth and survival: application to proliferation and cytotoxicity assays. *J Immunol Methods* **65**, 55–63.
27. Carmichael J, Degraff WG, Gazdar AF, Minna JD, Mitchell JB (1987) Evaluation of a tetrazolium-based semiautomated colorimetric assay: assessment of a chemosensitivity testing. *Cancer Res* **47**, 936–942.
28. Doyly A, Griffiths JB (1997) *Mammalian Cell Culture-essential Techniques*, John Wiley & Sons, Chichester, UK.
29. Morris GM, Huey R, Lindstrom W, Sanner MF, Belew RK, Goodsell DS, Olson AJ (2009) AutoDock4 and AutoDockTools4: Automated docking with selective receptor flexibility. *J Comput Chem* **30**, 2785–2791.
30. Jadhav AK, Karuppayil SM (2017) Molecular docking studies on thirteen fluoroquinolines with human topoisomerase II a and b. *In Silico Pharmacol* **5**, 4–15.
31. Sy LK, Brown GD (1997) Total assignment of the ^{1}H and ^{13}C NMR chemical shifts of three bisabolane hydrocarbons by 2D-NMR spectroscopy. *Magn Reson Chem* **35**, 424–425.
32. Wongkanya R, Teeranachaideekul V, Makarasen A, Chuysinuan P, Yingyuad P, Nooeaid P, Techasakul S, Chuenchom L, et al (2020) Electrospun poly(lactic acid) nanofiber mats for controlled transdermal delivery of essential oil from *Zingiber cassumunar* Roxb. *Mater Res Express* **7**, ID 055305.
33. Masuda T, Andoh T, Yonemori S, Takeda Y (1999) Phenylbutenoids from the rhizomes of *Alpinia abellata*. *Phytochemistry* **50**, 163–166.
34. Lu Y, Liu R, Berthod A, Pan Y (2008) Rapid screening of bioactive components from *Zingiber cassumunar* using elution-extrusion counter-current chromatography. *J Chromatogr A* **1181**, 33–44.
35. Pendleton MJ, Lindsey RH, Felix CA, Grimwade D, Osheroff N (2014) Topoisomerase II and leukemia. *Ann NY Acad Sci* **1310**, 98–110.
36. Felix CA (2001) Leukemias related to treatment with DNA Topoisomerase II inhibitors. *Med Pediatr Oncol* **36**, 525–535.
37. Boshoff C, Begent RH, Oliver RT, Rustin GJ, Newlands ES, Andrews R, Skelton M, Holden L, et al (1995) Secondary tumours following etoposide containing therapy for germ cell cancer. *Ann Oncol* **8**, 35–40.
38. Congras A, Caillet N, Torossian N, Quelen C, Daugrois C, Brousset P, Lamant L, Meggetto F, et al (2018) Doxorubicin-induced loss of DNA topoisomerase II and DNMT1-dependent suppression of MiR-125b induces chemoresistance in ALK-positive cells. *Oncotarget* **9**, 14539–14551.
39. McClendon AK, Osheroff N (2007) DNA topoisomerase II, genotoxicity, and cancer. *Mutat Res* **623**, 83–97.
40. Nitiss JL (2009) Targeting DNA topoisomerase II in cancer chemotherapy. *Nat Rev Cancer* **9**, 338–350.

Appendix A. Supplementary data

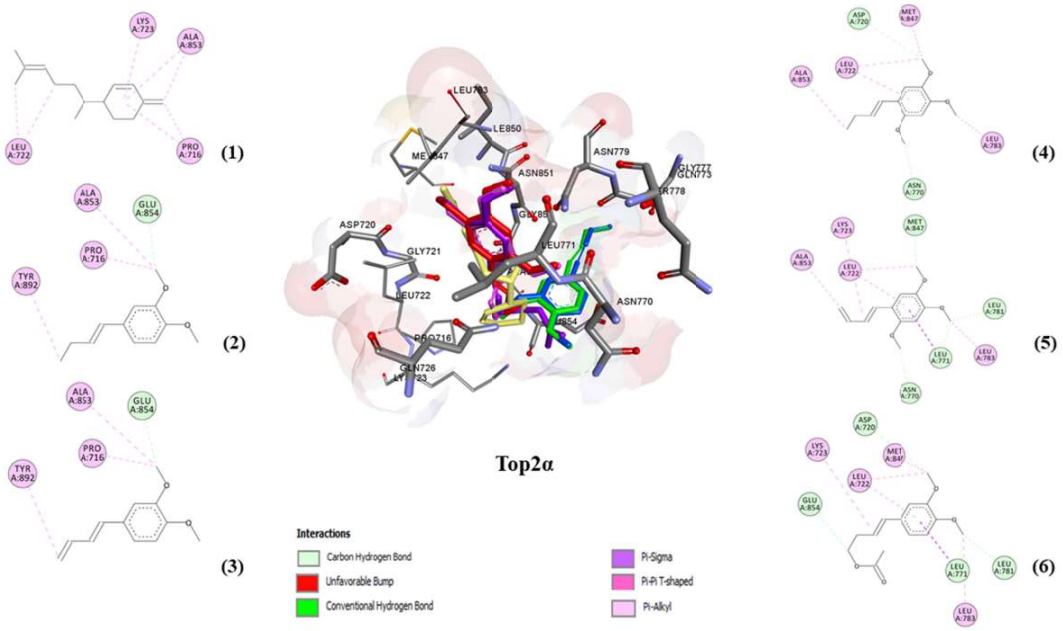

Fig. S1 The binding interaction between the ligands ((1): yellow, (2): green, (3): blue, (4): red, (5): pink, (6): purple) and Top2α using molecular docking.

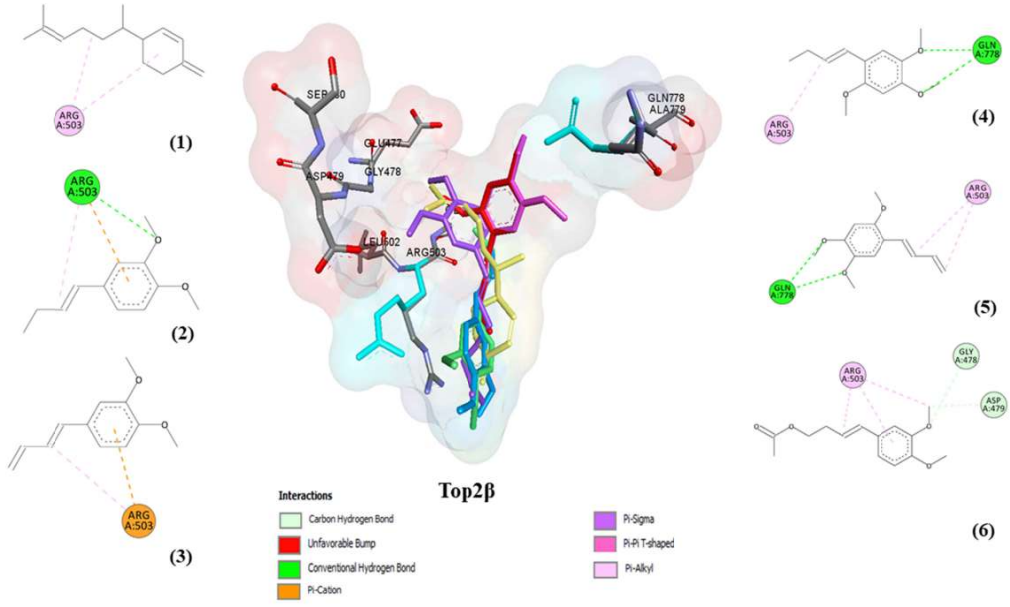

Fig. S2 The binding interaction between the ligands ((1): yellow, (2): green, (3): blue, (4): red, (5): pink, (6): purple) and Top2β using molecular docking.

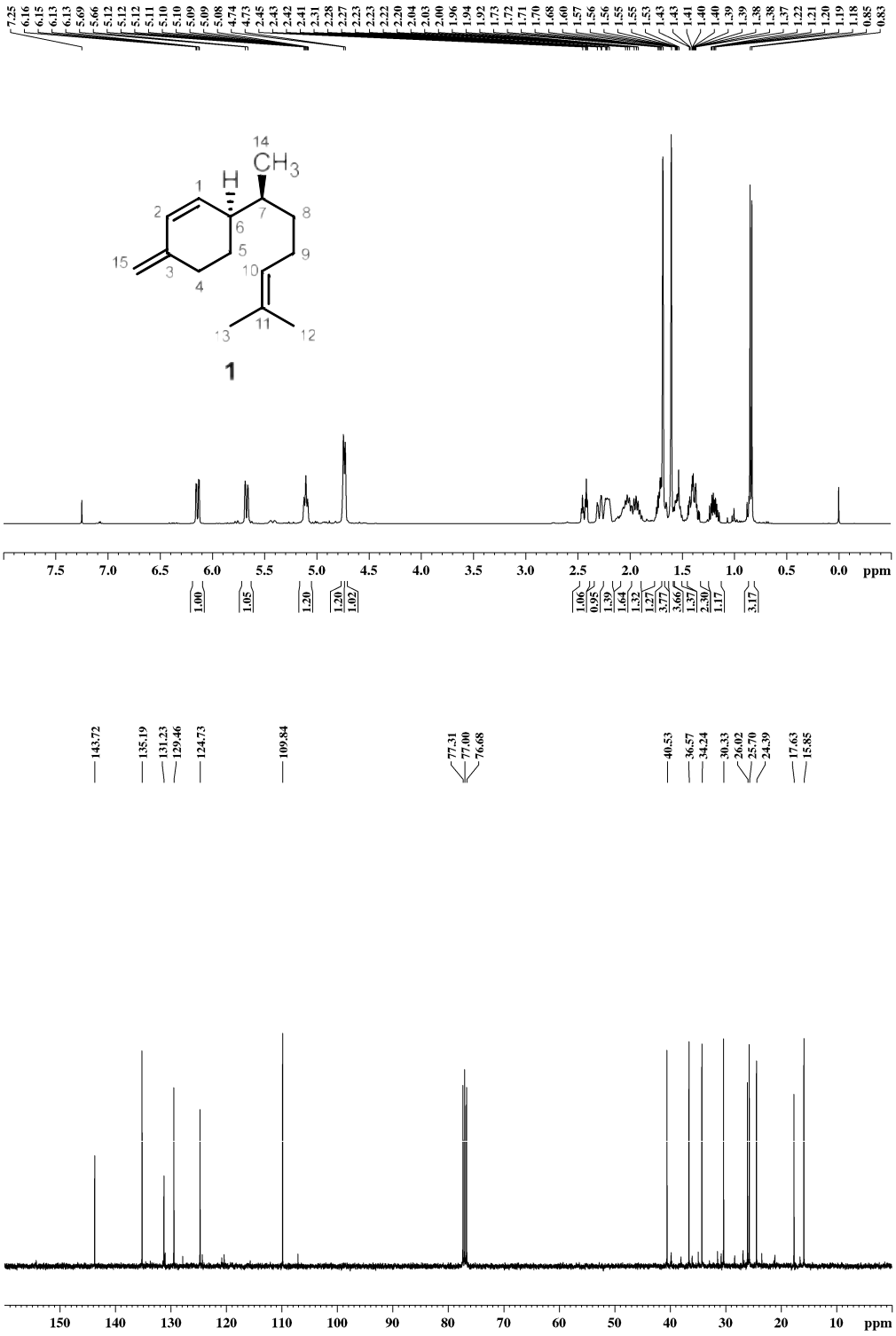

Fig. S3 ^{1}H-NMR ($CDCl_3$, 400 MHz) and ^{13}C-NMR ($CDCl_3$, 100 MHz) spectra of 1.

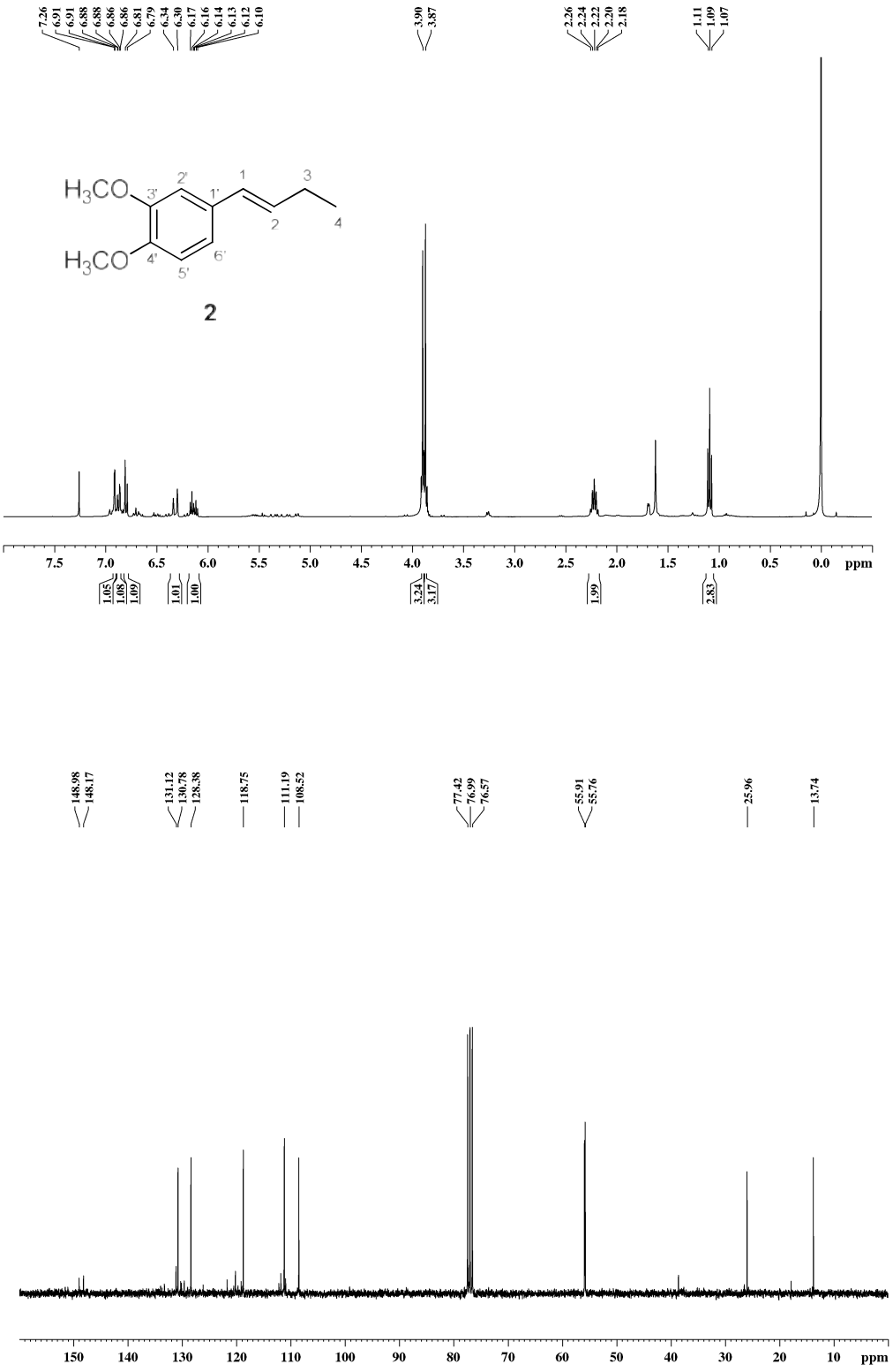

Fig. S4 ^{1}H-NMR ($CDCl_3$, 400 MHz) and ^{13}C-NMR ($CDCl_3$, 100 MHz) spectra of 2.

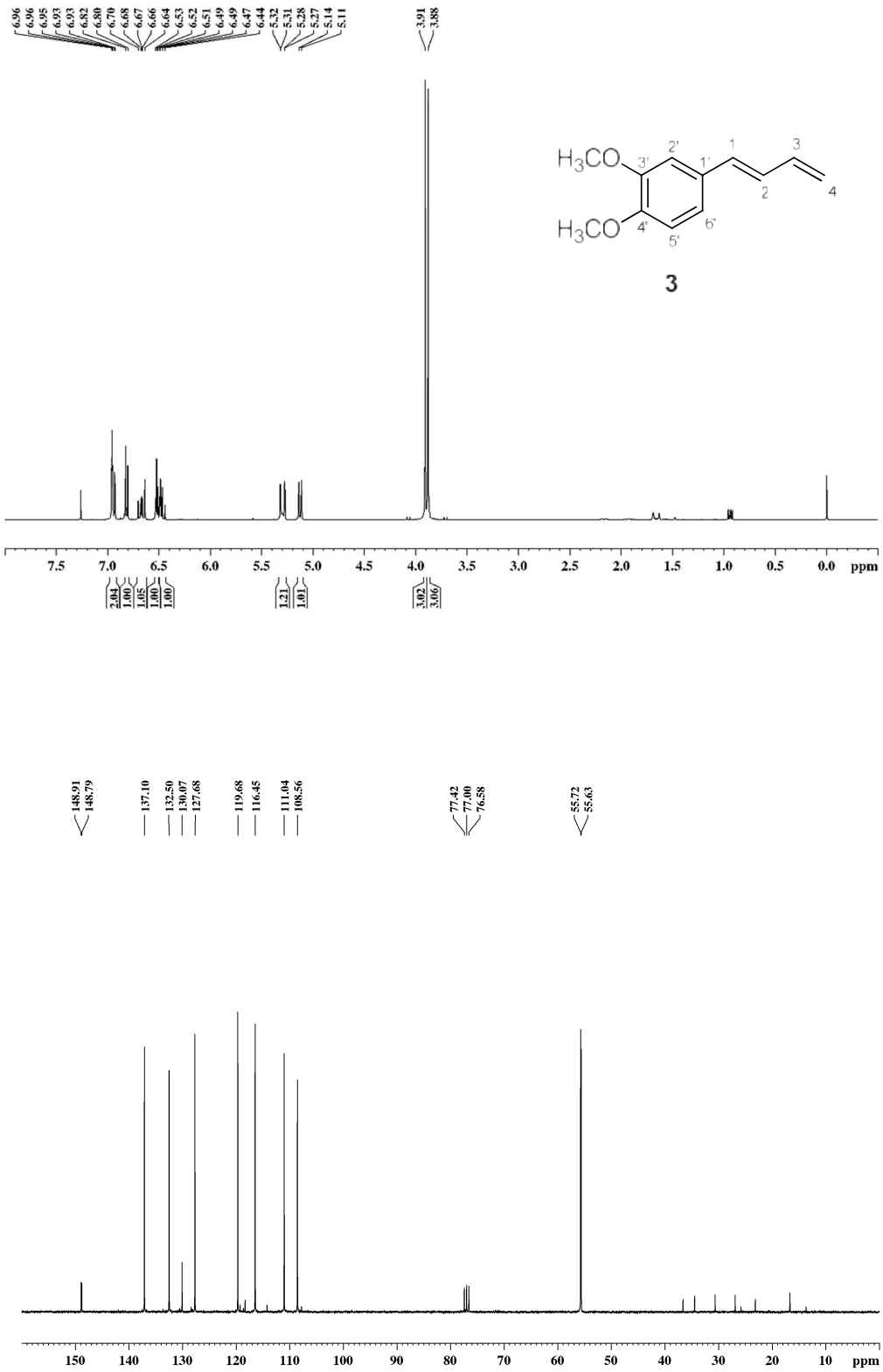

Fig. S5 ^{1}H-NMR ($CDCl_3$, 400 MHz) and ^{13}C-NMR ($CDCl_3$, 100 MHz) spectra of 3.

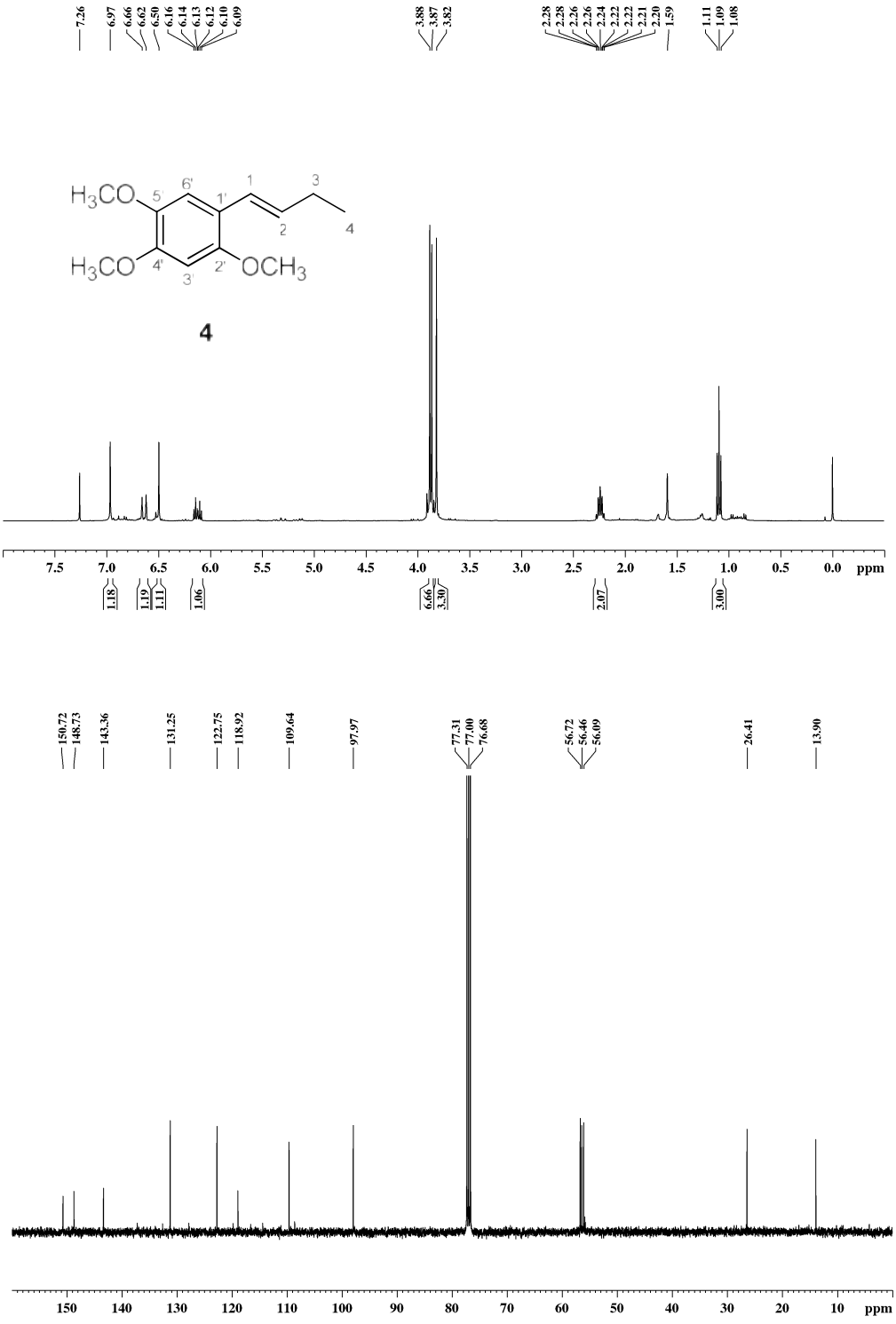

Fig. S6 ^{1}H-NMR ($CDCl_3$, 400 MHz) and ^{13}C-NMR ($CDCl_3$, 100 MHz) spectra of 4.

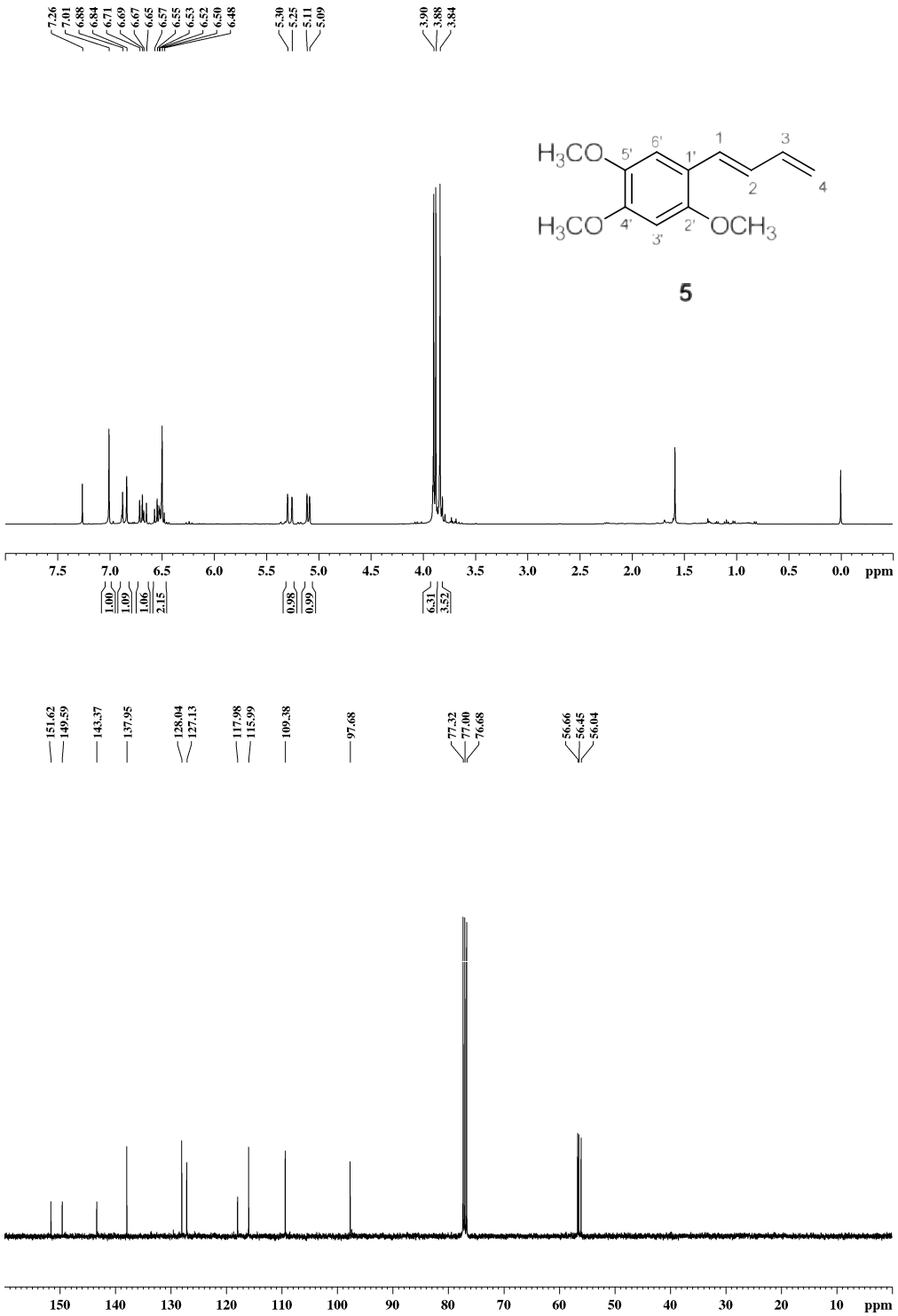

Fig. S7 ^{1}H-NMR ($CDCl_3$, 400 MHz) and ^{13}C-NMR ($CDCl_3$, 100 MHz) spectra of 5.

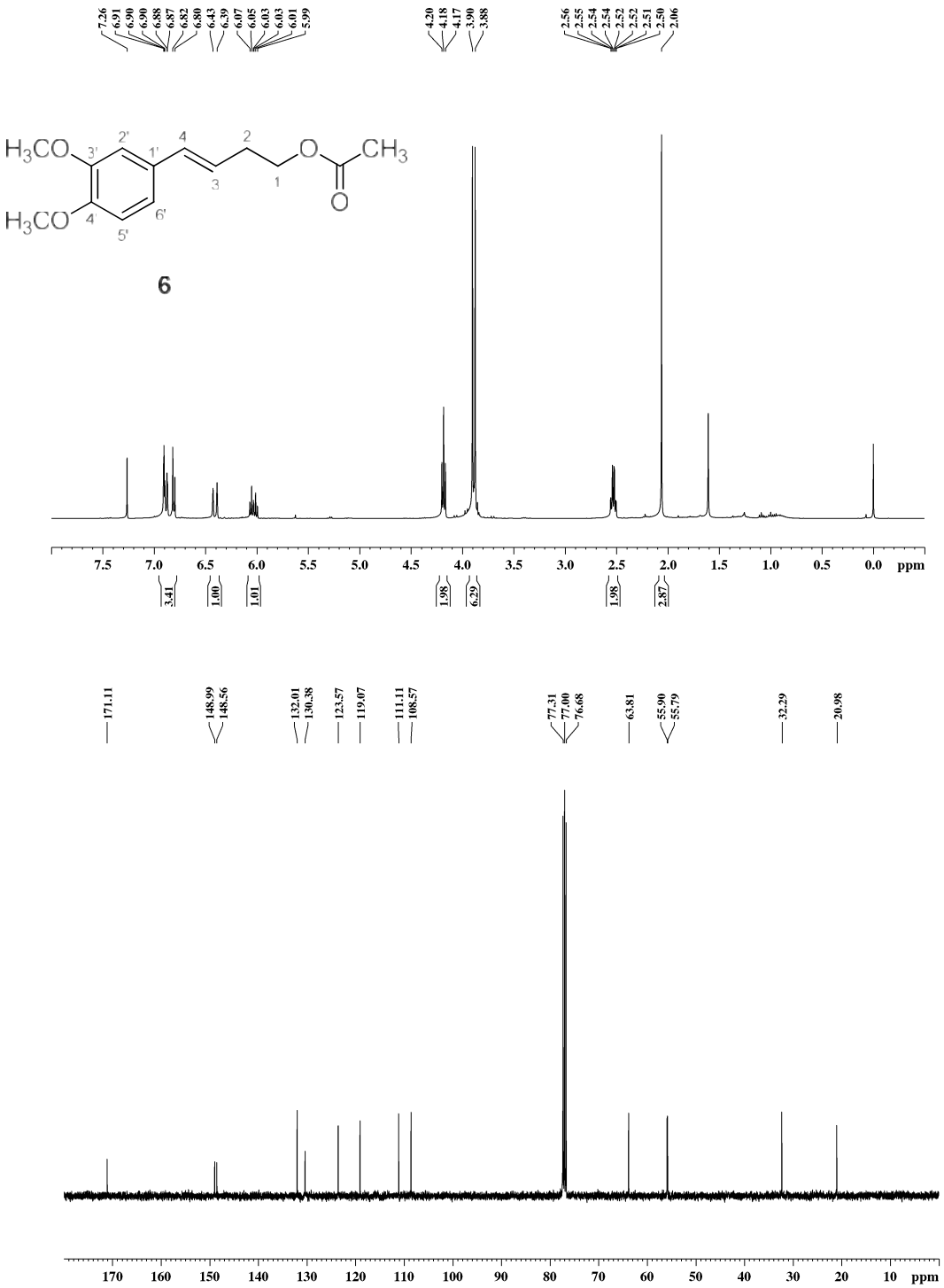

Fig. S8 ^{1}H-NMR ($CDCl_3$, 400 MHz) and ^{13}C-NMR ($CDCl_3$, 100 MHz) spectra of 6.

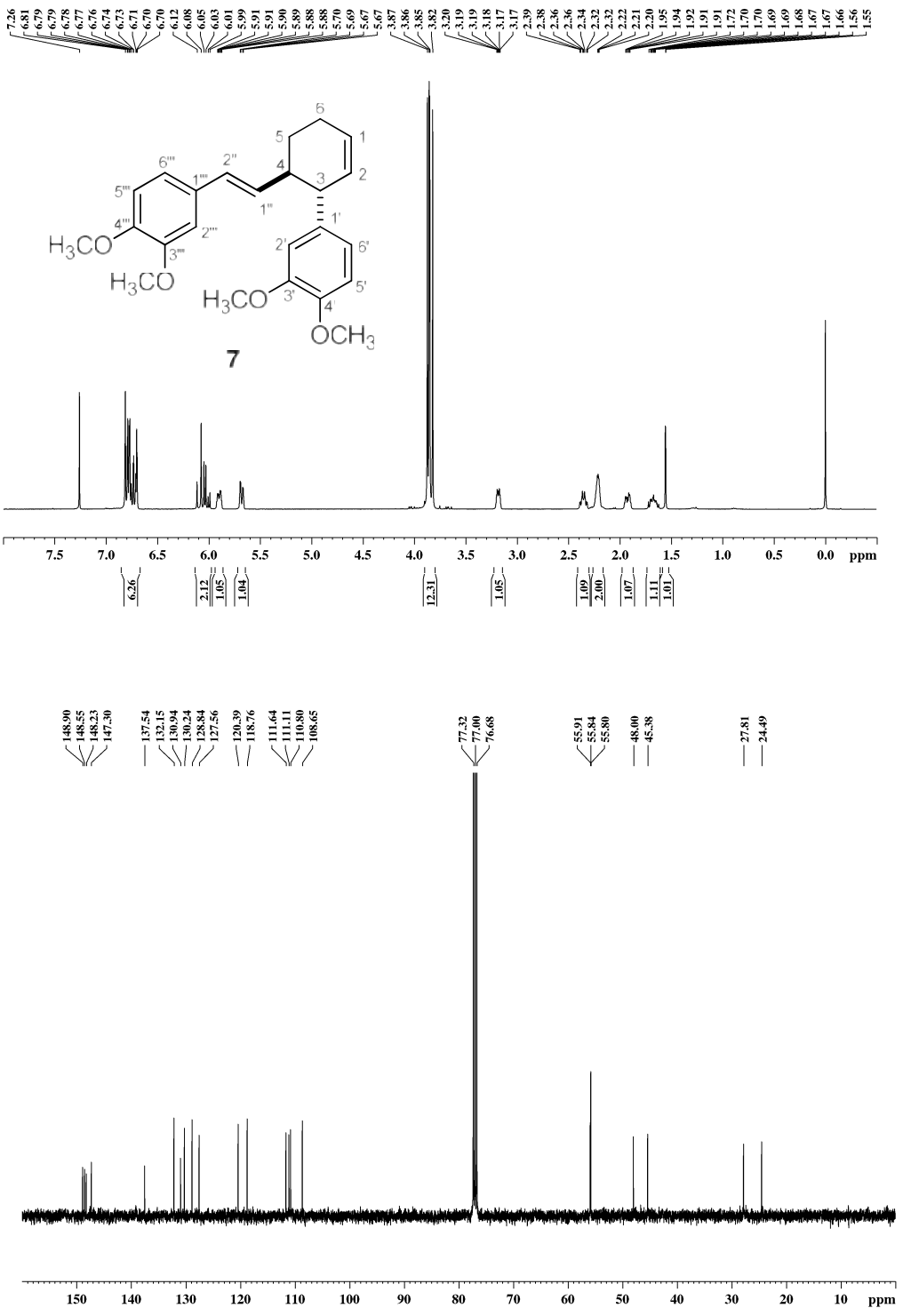

Fig. S9 ^{1}H-NMR ($CDCl_3$, 400 MHz) and ^{13}C-NMR ($CDCl_3$, 100 MHz) spectra of 7.

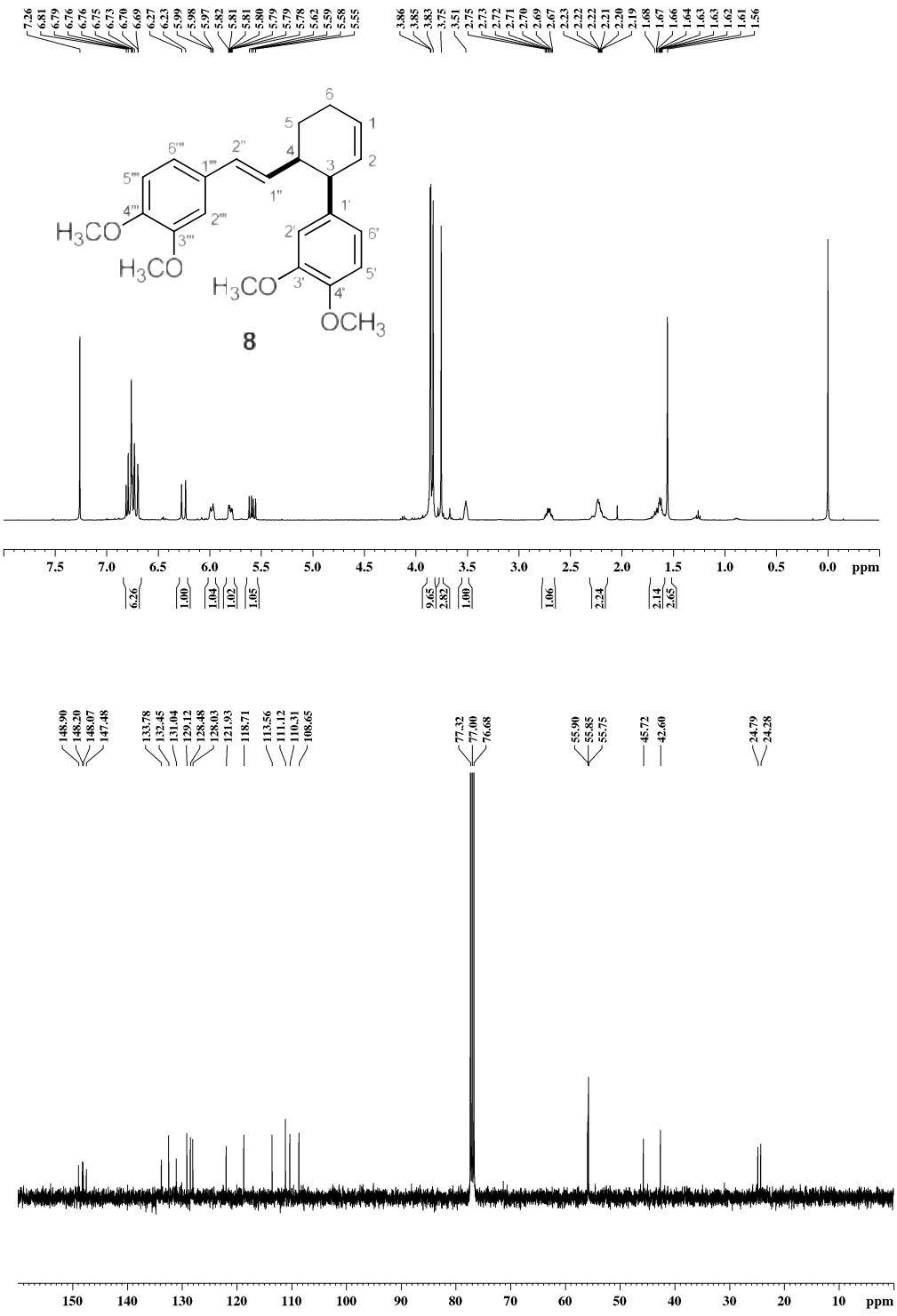

Fig. S10 ^{1}H-NMR ($CDCl_3$, 400 MHz) and ^{13}C-NMR ($CDCl_3$, 100 MHz) spectra of 8.

Table S1 NMR spectroscopic data of compounds 1.

Pos.	**1**	
	^{1}H (ppm, multiplicity, *J* (Hz))	^{13}C (ppm)
1	5.67, d, 10.0	135.2
2	6.14, dd, 10.0, 2.4	129.5
3	–	143.7
4	2.27–2.31, m 2.44, dt, 14.8,4.0	30.3
5	1.33–1.44, m 1.70–1.75, m	24.4
6	2.20–2.24, m	40.5
7	1.50–1.58, m	36.6
8	1.14–1.24, m 1.33–1.44, m	34.2
9	1.90–1.99, m 1.99–2.06, m	26.0
10	5.10, tt, 7.2, 1.2	124.7
11	–	131.2
12	1.60, s	17.6
13	1.69, s	25.7
14	0.84, d, 6.8	15.8
15	4.73, s 4.75, s	109.8

Table S2 ^{1}H NMR spectroscopic data of compounds 2–6.

Pos.	δ (ppm), multiplicity, *J* (Hz)				
	2	**3**	**4**	**5**	**6**
1	6.32, d, 16.0	6.51–6.53, m	6.64, d, 16.0	6.86, d, 15.6	4.18, t, 6.8
2	6.14, dt, 16.0, 8.0	6.67, dd, 15.2, 10.8	6.12, dt, 16.0, 6.8	6.68, dd, 15.6, 10.0	2.53, qd, 6.8, 1.2
3	2.23, qn, 8.0	6.44–6.49, m	2.24, qnd, 7.6, 1.6	6.48–6.57, m	6.03, dt, 16.0, 6.8
4	1.09, t, 8.0	H_a: 5.13, d, 9.7 H_b: 5.30, dd, 16.4, 1.6	1.10, t, 7.2	H_a: 5.10, d, 10.0 H_b: 5.28, d, 16.8	6.41, d, 16.0
1′	–	–	–	–	–
2′	6.91, d, 2.0	6.93–6.96, m	–	–	6.87–6.91, m
3′	–	–	6.50, s 6.50, s	–	
4′	–	–	–	–	–
5′	6.80, d, 8.0	6.82, d, 8.0	–	–	6.81, d, 8.0
6′	6.87, dd, 8.0, 2.0	6.93–6.96, m	6.97, s	7.00, s	6.87–6.91, m
OMe	3.87, s	3.88, s	3.82, s	3.84, s	3.88, s
	3.90, s	3.91, s	3.87, s	3.88, s	3.90, s
	–	–	3.88, s	3.90, s	–
OAc	–	–	–	–	2.06, s

Table S3 ^{13}C NMR spectroscopic data of compounds 2–6.

Pos.	^{13}C (ppm)				
	2	**3**	**4**	**5**	**6**
1	130.7	132.6	131.3	138.0	63.8
2	128.4	127.8	122.8	128.0	32.3
3	26.0	137.2	26.4	127.1	123.6
4	13.7	116.6	13.9	116.0	132.0
1′	131.1	130.2	118.9	118.0	130.4
2′	108.4	108.5	143.4	143.4	108.6
3′	148.9	149.0	98.0	97.7	149.0
4′	148.1	148.8	150.7	151.6	148.6
5′	111.1	110.1	148.7	149.6	111.1
6′	118.7	119.8	109.6	109.4	119.1
OMe	55.7	55.8	56.1	56.0	55.8
	55.9	55.9	56.5	56.5	55.9
	–	–	56.7	56.7	–
OAc	–	–	–	–	21.0
					171.1

Table S4 NMR spectroscopic data of compounds 7 and 8.

Pos.	^{1}H (ppm, multiplicity, *J* (Hz))		^{13}C (ppm)	
	7	**8**	**7**	**8**
1	5.88–5.92, m	5.97–5.99, m	127.6	128.0
2	5.68, dd, 10.0	2.4 5.78–5.82, m	130.2	129.1
3	3.17–3.20, m	3.51, bs	48.0	45.7
4	2.32–2.39, m	2.67–2.75, m	45.4	42.6
5	H_a: 1.66–1.72, m H_b: 1.90–1.96, m	1.61–1.68, m	27.8	24.3
6	2.20–2.22, m	2.19–2.23, m	24.5	24.8
1′	–	–	137.5	133.8
2′	6.70–6.81, m	6.69–6.81, m	111.6	113.6
3′	–	–	147.3*	147.5*
4′	–	–	148.2*	148.1*
5′	6.70–6.81, m 6.69–6.81, m	110.8	110.3	
6′	6.70–6.81, m 6.69–6.81, m	120.4	121.9	
1″	6.01, dd, 16.0, 6.8	5.59, dd, 15.6, 9.2	132.2	132.4
2″	6.10, d, 16.0	6.25, d, 15.6	128.8	128.5
1‴	–	–	130.9	131.0
2‴	6.70–6.81, m	6.69–6.81, m	108.7	108.6
3‴	–	–	148.6*	148.2*
4‴	–	–	148.9*	148.9*
5‴	6.70–6.81, m	6.69–6.81, m	111.1	111.1
6‴	6.70–6.81, m	6.69–6.81, m	118.8	118.7
OMe	3.82, s	3.75, s	55.8	55.7
	3.85, s	3.83, s	55.8	55.8
	3.86, s	3.85, s	55.9	55.9
	3.87, s	3.86, s	24.5	24.8

* Uncertain position because of the $-OCH_3$ groups.